

Multifractal analysis of fluid particle accelerations in turbulence

Toshihico Arimitsu^a and Naoko Arimitsu^b

^a*Institute of Physics, University of Tsukuba, Ibaraki 305-8571, Japan*

^b*Graduate School of EIS, Yokohama Nat'l. University, Yokohama 240-8501, Japan*

Abstract

The probability density function (PDF) of accelerations in turbulence is derived analytically with the help of the multifractal analysis based on generalized entropy, i.e., the Tsallis or the Rényi entropy. It is shown that the derived PDF explains quite well the one obtained by Bodenschatz et al. in the measurement of fluid particle accelerations in the Lagrangian frame at $R_\lambda = 690$, and the one by Gotoh et al. in the DNS with the mesh size 1024^3 at $R_\lambda = 380$.

Key words: multifractal analysis, fully developed turbulence, PDF of fluid particle accelerations, Rényi entropy, Tsallis entropy

PACS: 47.27.-i, 47.53.+n, 47.52.+j, 05.90.+m

1 Introduction

The *multifractal analysis* of turbulence [1,2,3,4,5,6,7,8,9,10] is a unified self-consistent approach for the systems with large deviations, which has been constructed based on the Tsallis-type distribution function [11,12] that provides an extremum of the *extensive* Rényi [13] or the *non-extensive* Tsallis entropy [11,12,14] under appropriate constraints. The analysis rests on the scale invariance of the Navier-Stokes equation for high Reynolds number, and on the assumptions that the singularities due to the invariance distribute themselves multifractally in physical space. The multifractal analysis belongs to the line of study based on a kind of *ensemble* theoretical approaches that, starting from K41 [15], continues with the log-normal model [16,17,18], the β -model [19], the p-model [20,21], the 3D binomial Cantor set model [22] and so on.

Email address: arimitsu@cm.ph.tsukuba.ac.jp (Toshihico Arimitsu).

After a rather preliminary investigation of the p-model [1], we developed further to derive the analytical expression for the scaling exponents of velocity structure function [2,3,4,5], and to determine the probability density function (PDF) of velocity fluctuations [5,6,7,8], of velocity derivative [9] and of fluid particle accelerations [10] by a self-consistent statistical mechanical approach. It has been shown [5] that the multifractal analysis derives the log-normal model [16,17,18] when one starts with the Boltzmann-Gibbs entropy.

In this paper, we derive the formula for the PDF of the accelerations of a fluid particle in fully developed turbulence by means of the multifractal analysis, and will analyze two experiments. One is the PDF of accelerations at $R_\lambda = 690$ of the Taylor microscale Reynolds number obtained in the Lagrangian measurement of particle accelerations that was realized by Bodenschatz et al. [23,24,25] by raising dramatically the spatial and temporal measurement resolutions with the help of the silicon strip detectors. The other is the PDF of accelerations at $R_\lambda = 380$ [26] that was extracted by Gotoh from the DNS of the size 1024^3 [27] which may be the largest mesh size available at present.

For high Reynolds number $\text{Re} \gg 1$, or for the situation where effects of the kinematic viscosity ν can be neglected compared with those of the turbulent viscosity, the Navier-Stokes equation,

$$\partial \vec{u} / \partial t + (\vec{u} \cdot \vec{\nabla}) \vec{u} = -\vec{\nabla} (p/\rho) + \nu \nabla^2 \vec{u}, \quad (1)$$

of an incompressible fluid is invariant under the scale transformation [28,21]

$$\vec{r} \rightarrow \lambda \vec{r}, \quad \vec{u} \rightarrow \lambda^{\alpha/3} \vec{u}, \quad t \rightarrow \lambda^{1-\alpha/3} t, \quad (p/\rho) \rightarrow \lambda^{2\alpha/3} (p/\rho) \quad (2)$$

where the exponent α is an arbitrary real quantity. The quantities ρ and p represent, respectively, mass density and pressure. The acceleration \vec{a} of a fluid particle is given by the substantive time derivative of the velocity:

$$\vec{a} = \partial \vec{u} / \partial t + (\vec{u} \cdot \vec{\nabla}) \vec{u}. \quad (3)$$

The Reynolds number Re of the system is given by

$$\text{Re} = \delta u_{\text{in}} \ell_{\text{in}} / \nu = (\ell_{\text{in}} / \eta)^{4/3} \quad (4)$$

with the Kolmogorov scale $\eta = (\nu^3 / \epsilon)^{1/4}$ [15] where ϵ is the energy input rate at the *energy-input* scale ℓ_{in} . The velocity fluctuation δu_{in} is defined by putting $\ell_n = \ell_{\text{in}}$ in $\delta u_n = |u(\bullet + \ell_n) - u(\bullet)|$ where u is a component of velocity field \vec{u} , and ℓ_n is a distance between two observing points. We are measuring distance

by the discrete units

$$\ell_n = \delta_n \ell_0 \quad (5)$$

with $\delta_n = 2^{-n}$ ($n = 0, 1, 2, \dots$) and ℓ_0 being some reference length. The non-negative integer n represents the *multifractal depth*. However, we will treat it as positive real number in the analysis of experiments.

It may be worthwhile to note here that, within the energy cascade model, the diameter $\ell_{\bar{n}}$ of eddies should be defined by

$$\ell_{\bar{n}} = \delta_{\bar{n}} \ell_{\text{in}}. \quad (6)$$

Therefore, if one identifies the distance ℓ_n with the diameter $\ell_{\bar{n}}$ of the \bar{n} th eddies within the energy cascade model, one has the relation

$$\bar{n} = n - \log_2 (\ell_0 / \ell_{\text{in}}) \quad (7)$$

between the number n of the multifractal steps and the number \bar{n} of the steps within the energy cascade. We see that $\ell_{\text{in}} = \ell_0$ as it should be.

Introducing the *pressure* (divided by the mass density) difference

$$\delta p_n = |p/\rho(\bullet + \ell_n) - p/\rho(\bullet)| \quad (8)$$

between two points separated by the distance ℓ_n , the accelerations may be estimated by

$$|\vec{a}| = \lim_{n \rightarrow \infty} a_n \quad (9)$$

where we introduced the acceleration

$$a_n = \delta p_n / \ell_n \quad (10)$$

belonging to the multifractal depth n . The acceleration becomes singular for $\alpha < 1.5$, i.e.,

$$\lim_{n \rightarrow \infty} a_n = \lim_{\ell_n \rightarrow 0} \delta p_n / \ell_n \sim \lim_{\ell_n \rightarrow 0} \ell_n^{(2\alpha/3)-1} \rightarrow \infty \quad (11)$$

which can be seen with the relation

$$\delta p_n / \delta p_0 = (\ell_n / \ell_0)^{2\alpha/3}. \quad (12)$$

The values of exponent α specify the degree of singularity.

2 Multifractal spectrum

The multifractal analysis rests on the multifractal distribution of α . The probability $P^{(n)}(\alpha)d\alpha$ to find, at a point in physical space, a singularity labeled by an exponent in the range $\alpha \sim \alpha + d\alpha$ is given by [2,3,4,5]

$$P^{(n)}(\alpha) = Z_{\alpha}^{(n)-1} \left[1 - (\alpha - \alpha_0)^2 / (\Delta\alpha)^2 \right]^{n/(1-q)} \quad (13)$$

with an appropriate partition function $Z_{\alpha}^{(n)}$ and

$$(\Delta\alpha)^2 = 2X / [(1 - q) \ln 2]. \quad (14)$$

The range of α is $\alpha_{\min} \leq \alpha \leq \alpha_{\max}$ with

$$\alpha_{\min} = \alpha_0 - \Delta\alpha, \quad \alpha_{\max} = \alpha_0 + \Delta\alpha. \quad (15)$$

It may be worthwhile to put here its brief derivation in order to make the paper self-contained. The distribution function (13) is derived by taking an extremum of the generalized entropy, the Rényi entropy [13]

$$S_q^R[P^{(1)}(\alpha)] = (1 - q)^{-1} \ln \int d\alpha P^{(1)}(\alpha)^q \quad (16)$$

or the Tsallis entropy [11,12,14]

$$S_q^T[P^{(1)}(\alpha)] = (1 - q)^{-1} \left(\int d\alpha P^{(1)}(\alpha)^q - 1 \right), \quad (17)$$

under the two constraints, i.e., the normalization of distribution function:

$$\int d\alpha P^{(1)}(\alpha) = \text{const.}, \quad (18)$$

and the q -variance being kept constant as a known quantity:

$$\sigma_q^2 = \left(\int d\alpha P^{(1)}(\alpha)^q (\alpha - \alpha_0)^2 \right) / \int d\alpha P^{(1)}(\alpha)^q. \quad (19)$$

Here, we assume that the distribution function at the n th multifractal depth has the structure

$$P^{(n)}(\alpha) \propto [P^{(1)}(\alpha)]^n. \quad (20)$$

This is consistent with the relation [21,5]

$$P^{(n)}(\alpha) \propto \delta_n^{1-f(\alpha)} \quad (21)$$

that is a manifestation of scale invariance and reveals how densely each singularity, labeled by α , fills physical space. In the present model, the multifractal spectrum $f(\alpha)$ is given by [2,3,4,5]

$$f(\alpha) = 1 + (1 - q)^{-1} \log_2 [1 - (\alpha - \alpha_0)^2 / (\Delta\alpha)^2]. \quad (22)$$

In spite of the different characteristics of these entropies, i.e., extensive and non-extensive, the distribution functions giving their extremum have the common structure (13).¹

The dependence of the parameters α_0 , X and q on the intermittency exponent μ is determined, self-consistently, with the help of the three independent equations, i.e., the energy conservation:

$$\langle \epsilon_n \rangle = \epsilon, \quad (23)$$

the definition of the intermittency exponent μ :

$$\langle \epsilon_n^2 \rangle = \epsilon^2 \delta_n^{-\mu}, \quad (24)$$

and the scaling relation²:

$$1/(1 - q) = 1/\alpha_- - 1/\alpha_+ \quad (25)$$

with α_{\pm} satisfying $f(\alpha_{\pm}) = 0$. The average $\langle \dots \rangle$ is taken with $P^{(n)}(\alpha)$. The energy-transfer rate ϵ_n represents the rate of transfer of energy per unit mass from eddies of size $\ell_n = \ell_{\bar{n}}$ (the \bar{n} th step within the energy cascade model) to those of size $\ell_{n+1} = \ell_{\bar{n+1}}$ (the $\bar{n+1}$ th step within the energy cascade model).

¹ Within the present formulation, the decision cannot be pronounced which of the entropies is underlying the system of turbulence.

² The scaling relation is a generalization of the one derived first in [29,30] to the case where the multifractal spectrum has negative values.

It should be noted that the average $\langle \epsilon_n \rangle$ is taken just for the eddies having the size ℓ_n . It is *not* the average within the spatial region of the diameter ℓ_n .

For the region $0.13 \leq \mu \leq 0.40$ where the value of μ is usually observed, the three self-consistent equations are solved to give the approximate equations [8]:

$$\alpha_0 = 0.9989 + 0.5814\mu, \quad X = -2.848 \times 10^{-3} + 1.198\mu \quad (26)$$

$$q = -1.507 + 20.58\mu - 97.11\mu^2 + 260.4\mu^3 - 365.4\mu^4 + 208.3\mu^5. \quad (27)$$

3 Scaling exponent of velocity structure function

Let us derive first the probability $\Lambda^{(n)}(y_n)dy_n$ to find the scaled pressure fluctuations

$$|y_n| = \delta p_n / \delta p_0 \quad (28)$$

in the range $y_n \sim y_n + dy_n$ in the form

$$\Lambda^{(n)}(y_n)dy_n = \Lambda_S^{(n)}(y_n)dy_n + \Delta\Lambda^{(n)}(y_n)dy_n \quad (29)$$

with the normalization

$$\int_{-\infty}^{\infty} dy_n \Lambda^{(n)}(y_n) = 1. \quad (30)$$

Here, we assumed that it has two contributions whose origins are independent with each other. The first term represents the contribution by the singular part of accelerations stemmed from the multifractal distribution of the singularities in physical space. This is given by

$$\Lambda_S^{(n)}(|y_n|)dy_n \propto P^{(n)}(\alpha)d\alpha \quad (31)$$

with the transformation of the variables, $|y_n| = \delta_n^{2\alpha/3}$. Whereas the second term $\Delta\Lambda^{(n)}(y_n)dy_n$ represents the contribution from the dissipative term in the Navier-Stokes equation, and/or the one from the errors in measurements. The dissipative term has been discarded in the above investigation since it violates the invariance under the scale transformation. The contribution of the second term provides a correction to the first one. Note that the proportionality coefficient in (31) determines the portion of the contribution among

these two independent origins.³

The m th moments of the pressure fluctuations, $\langle\langle |y_n|^m \rangle\rangle$, are given by

$$\langle\langle |y_n|^m \rangle\rangle \equiv \int_{-\infty}^{\infty} dy_n |y_n|^m \Lambda^{(n)}(y_n) = 2\tilde{\gamma}_m^{(n)} + (1 - 2\tilde{\gamma}_0^{(n)}) a_{2m} \delta_n^{\zeta_{2m}} \quad (32)$$

where

$$2\tilde{\gamma}_m^{(n)} = \int_{-\infty}^{\infty} dy_n |y_n|^m \Delta \Lambda^{(n)}(y_n) \quad (33)$$

$$a_{3\bar{q}} = \{2/[\sqrt{C_{\bar{q}}}(1 + \sqrt{C_{\bar{q}}})]\}^{1/2} \quad (34)$$

with

$$C_{\bar{q}} = 1 + 2\bar{q}^2(1 - q)X \ln 2. \quad (35)$$

The quantity

$$\zeta_m = \alpha_0 m/3 - 2Xm^2/[9(1 + C_{m/3}^{1/2})] - [1 - \log_2(1 + C_{m/3}^{1/2})]/(1 - q) \quad (36)$$

is the scaling exponent of the m th order velocity structure function which explains successfully the experimental results [2,3,4,5]. Note that the formula is independent of n .

4 PDF of the fluid particle accelerations

We now derive the PDF, $\hat{\Lambda}^{(n)}(\omega_n)$, defined by the relation

$$\hat{\Lambda}^{(n)}(\omega_n) d\omega_n = \Lambda^{(n)}(y_n) dy_n \quad (37)$$

with the *acceleration* ω_n normalized by its deviation, i.e.,

$$|\omega_n| = a_n/\langle\langle a_n^2 \rangle\rangle^{1/2} = p_n/\langle\langle p_n^2 \rangle\rangle^{1/2} = y_n/\langle\langle y_n^2 \rangle\rangle^{1/2} = \bar{\omega}_n \delta_n^{2\alpha/3 - \zeta_4/2} \quad (38)$$

³ Needless to say that each term in (29) is a multiple of two PDF's, i.e., the PDF for one of the two independent origins to realize and the conditional PDF for a value y_n in the range $y_n \sim y_n + dy_n$ to come out. This is of course in a generalized sense in which the second correction term may weaken the first singular contribution.

with

$$\bar{\omega}_n = [2\tilde{\gamma}_2^{(n)}\delta_n^{-\zeta_4} + (1 - 2\tilde{\gamma}_0^{(n)})a_4]^{-1/2}. \quad (39)$$

It is reasonable to imagine that the origin of intermittent rare events is attributed to the singular term in (29). We then have, for the *tail part* $\omega_n^\dagger \leq |\omega_n| \leq \omega_n^{\max}$,

$$\begin{aligned} \hat{\Lambda}^{(n)}(\omega_n)d\omega_n &= \Lambda_S^{(n)}(y_n)dy_n \\ &= \tilde{\Lambda}_S^{(n)} \frac{\bar{\omega}_n}{|\omega_n|} \left[1 - \frac{1-q}{n} \frac{(3 \ln |\omega_n/\omega_{n,0}|)^2}{8X |\ln \delta_n|} \right]^{n/(1-q)} d\omega_n \end{aligned} \quad (40)$$

with

$$\omega_{n,0} = \bar{\omega}_n \delta_n^{2\alpha_0/3 - \zeta_4/2}, \quad \omega_n^{\max} = \bar{\omega}_n \delta_n^{2\alpha_{\min}/3 - \zeta_4/2} \quad (41)$$

and

$$\tilde{\Lambda}_S^{(n)} = 3 \left(1 - 2\tilde{\gamma}_0^{(n)} \right) / \left(4\bar{\omega}_n \sqrt{2\pi X |\ln \delta_n|} \right). \quad (42)$$

On the other hand, for smaller accelerations, the contribution to the PDF comes from both the singularity and thermal fluctuations or measurement error. We assume that this part of the PDF is described by Tsallis-type function with a new parameter q' , i.e., for the *center part* $|\omega_n| \leq \omega_n^\dagger$,

$$\begin{aligned} \hat{\Lambda}^{(n)}(\omega_n)d\omega_n &= \left[\hat{\Lambda}_S^{(n)}(y_n) + \Delta \hat{\Lambda}^{(n)}(y_n) \right] dy_n \\ &= \tilde{\Lambda}_S^{(n)} \left\{ 1 - \frac{1-q'}{2} \left[1 + \frac{3}{2} f'(\alpha^\dagger) \right] \left[\left(\frac{\omega_n}{\omega_n^\dagger} \right)^2 - 1 \right] \right\}^{1/(1-q')} d\omega_n. \end{aligned} \quad (43)$$

This specific form of the Tsallis function is determined by the condition that the two PDF's (40) and (43) should have the same value and the same slope at ω_n^\dagger which is defined by

$$\omega_n^\dagger = \bar{\omega}_n \delta_n^{2\alpha^\dagger/3 - \zeta_4/2} \quad (44)$$

with α^\dagger being the smaller solution of

$$\zeta_4/2 - 2\alpha/3 + 1 - f(\alpha) = 0. \quad (45)$$

It is the point at which $\hat{\Lambda}^{(n)}(\omega_n^\dagger)$ has the least n -dependence for large n .

With the help of the relation (43), we obtain $\Delta\Lambda^{(n)}(y_n)$, and have the formula to evaluate $\tilde{\gamma}_m^{(n)}$ in the form

$$2\tilde{\gamma}_m^{(n)} = \left(K_m^{(n)} - L_m^{(n)} \right) / \left(1 + K_0^{(n)} - L_0^{(n)} \right) \quad (46)$$

where

$$K_m^{(n)} = \frac{3 \delta_n^{2(m+1)\alpha^\dagger/3 - \zeta_4/2}}{2\sqrt{2\pi X |\ln \delta_n|}} \int_0^1 dz z^m \times \left[1 - \frac{1-q'}{2} \left[1 + \frac{3}{2} f'(\alpha^\dagger) \right] (z^2 - 1) \right]^{1/(1-q')}, \quad (47)$$

$$L_m^{(n)} = \frac{3 \delta_n^{2m\alpha^\dagger/3}}{2\sqrt{2\pi X |\ln \delta_n|}} \int_{z_{\min}}^1 dz z^{m-1} \left[1 - \frac{1-q}{n} \frac{(3 \ln |z/z_0^\dagger|)^2}{8X |\ln \delta_n|} \right]^{n/(1-q)} \quad (48)$$

with

$$z_{\min} = \omega_{\min}/\omega_n^\dagger = \delta_n^{2(\alpha_{\max} - \alpha^\dagger)/3}, \quad z_0^\dagger = \omega_{n,0}/\omega_n^\dagger = \delta_n^{2(\alpha_0 - \alpha^\dagger)/3}. \quad (49)$$

Now, the PDF of fluid particle accelerations, given by (40) and (43), is completely determined by three parameters, i.e., the intermittency exponent μ , the multifractal depth n which gives a characteristic length ℓ_n , and q' which appears in the Tsallis-type PDF at the center part. The intermittency exponent μ is determined by analyzing the measured scaling exponent ζ_m of the velocity structure function with the formula (36) as mentioned before.

As for the determination of the value n , the flatness of the PDF of fluid particle accelerations can be a good candidate [25]. Actually, the present multifractal analysis provides us with the analytical formula for the flatness of the PDF in the form

$$F_a^{(n)} \equiv \langle\langle a_n^4 \rangle\rangle / \langle\langle a_n^2 \rangle\rangle^2 = \langle\langle \omega_n^4 \rangle\rangle = \frac{2\tilde{\gamma}_4^{(n)} + (1 - 2\tilde{\gamma}_0^{(n)}) a_8 \delta_n^{\zeta_8}}{\left[2\tilde{\gamma}_2^{(n)} + (1 - 2\tilde{\gamma}_0^{(n)}) a_4 \delta_n^{\zeta_4} \right]^2} \quad (50)$$

$$\approx \frac{a_8}{(1 - 2\tilde{\gamma}_0^{(n)}) a_4^2} \delta_n^{\zeta_8 - 2\zeta_4}. \quad (51)$$

With this formula, the experimental value of the flatness $F_a^{(n)}$ gives the value of the multifractal step n . In deriving the approximate formula (51), we used the fact that the first terms both in the denominator and numerator of the last formula in (50) are two or three orders in magnitude smaller than the second terms. Note that the contribution to the flatness is mainly come from the tail

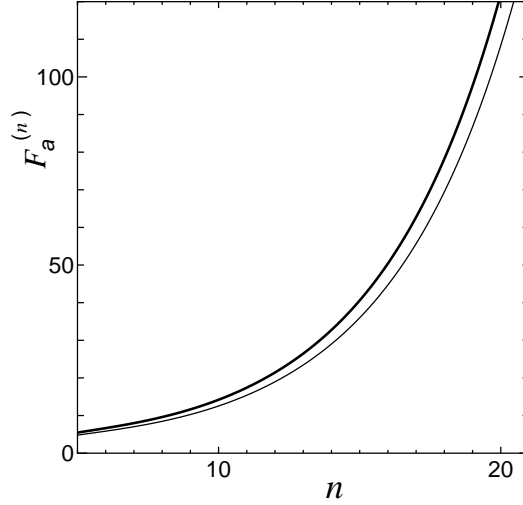


Fig. 1. Dependence of the flatness on the multifractal step n . The thin and thick lines represent, respectively, the dependence for the parameters used in the study of the experiment by Bodenschatz et al. (Fig. 2 below), and of the DNS by Gotoh et al. (Fig. 3 below).

part of the PDF, and that there is almost no contribution from its center part (see Fig. 4 below). Therefore, at this stage, we can determine almost the final shape and the magnitude of the tail part given by (40). It means that the shape of the center part, which is controlled by q' , rarely affect the tail part, and that the contribution of the center part to the normalization of PDF is almost independent of q' . The n -dependence of the flatness is given in Fig. 1 both for the cases corresponding to the experiments conducted by Bodenschatz et al. with the approximate formula

$$F_a^{(n)} = -6.872 + 5.216n - 9.969 \times 10^{-1}n^2 + 1.075 \times 10^{-1}n^3 - 5.296 \times 10^{-3}n^4 + 1.241 \times 10^{-4}n^5, \quad (52)$$

and to the DNS performed by Gotoh et al. with

$$F_a^{(n)} = -7.592 + 5.831n - 1.114n^2 + 1.203 \times 10^{-1}n^3 - 5.925 \times 10^{-3}n^4 + 1.389 \times 10^{-4}n^5. \quad (53)$$

The slight difference between the two formulae comes from the difference of the values q' (see Fig. 2 and Fig. 3 below).

Within the present stage of the multifractal analysis, the value q' is determined by adjusting the center part with the experimental data. However, since the center part of the PDF takes care only smaller accelerations compared with its deviation, we can expect that the dynamical analysis such as done by Beck [31,32] may be effective. The dynamical study for the center part will be

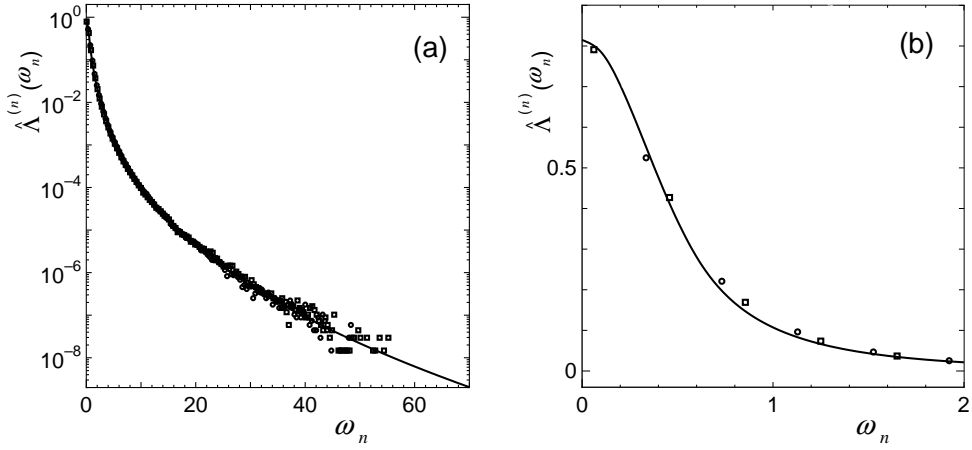


Fig. 2. PDF of accelerations plotted on (a) log and (b) linear scale. Comparison between the experimentally measured PDF of fluid particle accelerations by Bodenschatz et al. at $R_\lambda = 690$ ($Re = 31\,400$) and the present theoretical PDF $\hat{\Lambda}^{(n)}(\omega_n)$. Open squares are the experimental data points on the left hand side of the PDF, whereas open circles are those on the right hand side. Solid lines represent the curves given by the present theory (40) and (43) with $\mu = 0.240$ ($q = 0.391$), $n = 17.1$ and $q' = 1.45$.

reported elsewhere in connection with the multifractal characteristics of the system which determines the tail part representing large deviations.

5 Analysis of experiments

We analyze, with the formula (40) and (43), the experimental PDF at $R_\lambda = 690$ measured by Bodenschatz et al. [25] in Fig. 2 on (a) log and (b) linear scale. We determined the value $n = 17.1$ for this experiment by substituting into its definition (5), i.e., $n = \log_2(\ell_0/\ell_n)$, the reported value of the integral length scale 0.071 m for ℓ_0 , and of the spatial measurement resolution 0.5 μm for ℓ_n [23,24]. The intermittency exponent $\mu = 0.240$ is extracted by the method of least squares with respect to the logarithm of PDF's as the best fit of our theoretical formulae with $n = 17.1$ to the observed values of the PDF [23,24,25]. We discarded those points whose PDF values are less than $\sim 10^{-7}$ since they scatter largely on log scale. Substituting the extracted value of μ into the self-consistent equations, we have the values of parameters: $q = 0.391$, $\alpha_0 = 1.138$ and $X = 0.285$. With these values, other quantities are determined, e.g., $\Delta\alpha = 1.161$, $\alpha_+ - \alpha_0 = \alpha_0 - \alpha_- = 0.6815$, $\alpha^\dagger = 1.005$, $\omega_n^\dagger = 0.605$ and $\omega_n^{\max} = 2040$. The best fit at the center part is given with $q' = 1.45$.⁴ The

⁴ It is remarkable that this value of q' is close to $q' = 1.5$ proposed by Beck [31,32], although it is claimed that his formula does not provide a good explanation of

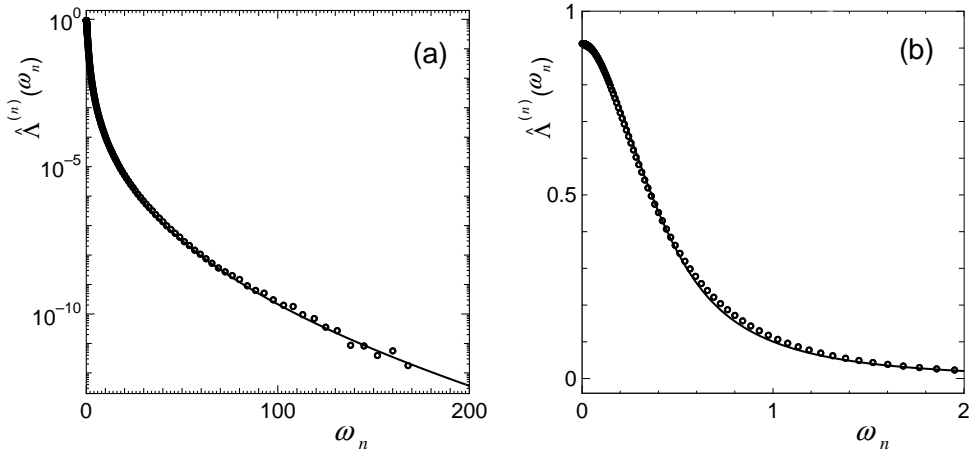


Fig. 3. PDF of accelerations plotted on (a) log and (b) linear scale. Comparison between the PDF of fluid particle accelerations measured in the DNS by Gotoh et al. at $R_\lambda = 380$ and the present theoretical PDF $\hat{\Lambda}^{(n)}(\omega_n)$. Closed circles are the DNS data points both on the left and right hand sides of the PDF. Solid lines represent the curves given by the present theory (40) and (43) with $\mu = 0.240$ ($q = 0.391$), $n = 17.5$ and $q' = 1.70$.

flatness of the PDF of accelerations has the value $F_a^{(n)} = 56.9$ which is within the reported value of the flatness 55 ± 4 [25]. This results tells us that the formula (50) of the flatness can be used to derive the value of μ , accurately, when one knows the value of n , and vice versa (see Fig. 1 and also Fig. 4 below).

Analysis of the PDF of accelerations extracted out from the DNS data obtained by Gotoh et al. [27] at $R_\lambda = 380$ is shown in Fig. 3 on (a) log and (b) linear scale. The value $\mu = 0.240$ for this DNS has been determined by the analysis of the experimental scaling exponent ζ_m of longitudinal velocity structure function with our theoretical formula (36) [8,9]. Substituting this value of μ into the self-consistent equations, we have the values of parameters: $q = 0.391$, $\alpha_0 = 1.138$, $X = 0.285$, $\Delta\alpha = 1.161$ and $\alpha_+ - \alpha_0 = \alpha_0 - \alpha_- = 0.6815$ which are the same as those derived in the analysis of the experiment by Bodenschatz, since both systems have a common value $\mu = 0.240$ for the intermittency exponent. The value $n = 17.5$ is extracted by the method of least squares with respect to the logarithm of PDF's as the best fit of our theoretical formulae with the derived parameters given above to the observed data of the PDF [27]. Note that $\alpha^\dagger = 1.005$, $\omega_n^\dagger = 0.622$ and $\omega_n^{\max} = 2534$. The best fit at the center part is given with $q' = 1.7$. The flatness of the PDF is $F_a^{(n)} = 70.0$. The characteristic distance $r = \ell_n$ for $n = 17.5$ reduces to $r/\eta = 7.91$ with $\eta \approx 0.258 \times 10^{-2}$ [27], which is about three times longer than the length $\Delta r/\eta = 2\pi/(1024\eta) = 2.38$ of the mesh of Gotoh's DNS. In

experimental PDF for larger accelerations [25].

deriving the characteristic distance, we used the second formula in⁵

$$n = -1.050 \log_2(r/\eta) + 16.74 \quad (\ell_c \leq r) \quad (54)$$

$$n = -2.540 \log_2(r/\eta) + 25.08 \quad (r < \ell_c). \quad (55)$$

Here, $\ell_c/\eta = 48.26$ is the crossover length of two scaling regions, and is close to the Taylor microscale $\lambda/\eta = 38.33$. With the help of the formula (7), we have $\bar{n} = 11.8$.

In Fig. 4, we put the lines representing the integrand $\omega_n^4 \hat{\Lambda}^{(n)}(\omega_n)$ of the flatness $F_a^{(n)}$ and the corresponding experimental data (a) by Bodenschatz et al. [25], and (b) by Gotoh et al. [27]. The agreements are remarkable.

6 Comment on the energy-input scale

There is no room to incorporate, *automatically*, into the present multifractal analysis the energy input scale ℓ_{in} and the "system size" ℓ_0 . The former is necessary to determine the number of steps \bar{n} in the energy cascade model. Once ℓ_{in} is determined by investigating the structure of experimental apparatuses, the relation between \bar{n} and the multifractal step n is given by (7). Since main part of the multifractal analysis rests on the scale invariance, the size of the system under consideration is assumed to be infinite, and therefore, the value of the reference length ℓ_0 introduced in (5) is determined only through the analysis of experimental data.

Actually, for example, the empirical equation [6]

$$n = -1.019 \log_2 r/\eta + 0.901 \log_2 \text{Re} \quad (56)$$

⁵ The empirical formulae (54) and (55) were extracted through the multifractal analysis for the PDF's of velocity fluctuations measured at two points separated by r [8]. The corresponding numbers n and \bar{n} are given by $(r/\eta, n, \bar{n}) = (2.38, 21.5, 14.5), (4.76, 20.0, 13.0), (9.52, 16.8, 9.81), (19.0, 14.0, 7.01), (38.1, 11.8, 4.81), (76.2, 10.1, 3.11), (152, 9.30, 2.31), (305, 8.10, 1.11), (609, 7.00, 0.01), (1220, 6.00, -0.99)$. It seems that there are two scaling regions constituting the inertial range. The formula (55) indicates that in the lower scaling region ($r < \ell_c$) eddies break up, effectively, into 1.33 pieces in contrast to the upper scaling region ($\ell_c \leq r$) where eddies break up into two pieces as seen in (54) [8]. The existence of the two scaling regions can be an artifact of DNS due to a shortage of calculation time, since energy cascading process is not so effective for eddies whose sizes are smaller than ℓ_c or the Taylor microscale. Note that Gotoh et al. claimed that the inertial range is restricted only to the region around $\bar{n} = 3.11, 2.31$ and 1.11 [27].

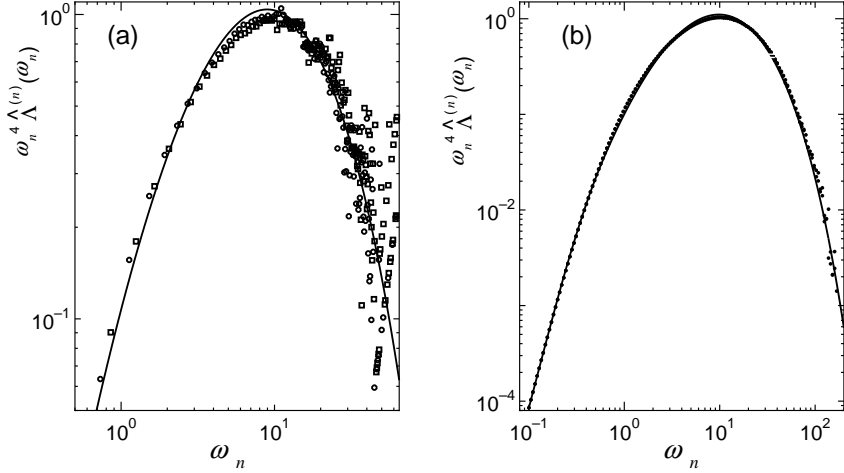


Fig. 4. Comparison of the theoretical curves (solid lines) for the integrand $\omega_n^4 \hat{\Lambda}^{(n)}(\omega_n)$ of the flatness $F_a^{(n)}$ with the corresponding (a) experimental quantity by Bodenschatz et al. (open squares for the data on the left hand side, and open circles on the right hand side), and (b) DNS quantity by Gotoh et al. (closed circles both for the data on the left and right hand) in loglog scale. The parameters in the theoretical PDF's for (a) and (b) are the same as those given in Fig. 2 and Fig. 3, respectively.

extracted from the experimental PDF's for velocity fluctuations⁶ by Lewis and Swinney [33] gives $\ell_0 \approx 877$ cm. In their analysis, the Reynolds number $Re = 540\,000$ is estimated with $\ell_{in} = 2\pi \times 19.00$ cm ≈ 119.32 cm and the Kolmogorov scale $\eta \approx 0.006$ cm. Therefore, the reference length is large compared with the energy-input scale.

For Gotoh's DNS, the empirical equation (54), extracted by the analysis of PDF's of velocity fluctuations, gives $\ell_0/\eta \approx 63\,000$ which is larger than the energy-input scale $\ell_{in}/\eta = \pi/(k\eta) \approx 497$ with the wavenumber $k = 6^{1/2}$ of forcing where we took 209 grid point spacings for the measure of the energy-input scale [34]. We see again that the reference length is longer than the energy-input scale. The Reynolds number of the DNS is now estimated by (4) as $Re = 3\,937$. A unified study of Gotoh's DNS [27] by means of the multifractal analysis with the Tsallis-type PDF for the center part will be given elsewhere, in which it is shown that the PDF's for the velocity fluctuations,

⁶ The velocity fluctuations are measured at two separated points whose distance is r . The corresponding numbers n and \bar{n} are given by [10] $(r/\eta, n, \bar{n}) = (11.6, 14, 10.7), (23.1, 13, 9.7), (46.2, 11, 8.7), (92.5, 10, 7.7), (208, 9.0, 6.6), (399, 8.0, 5.6), (830, 7.5, 4.6), (1440, 7.0, 3.8)$. The relation (56) is extracted with these values [6].

for the velocity derivatives and for the fluid particle accelerations in addition to the scale exponents of velocity structure function provide us with consistent results.

In the analysis of Bodenschatz's experiment, the identification of ℓ_0 with the integral length scale 7.1 cm gives us reasonable value of $n = 17.1$ in the sense that with this value the formula (50) of the flatness provides us with $\mu = 0.240$ for the intermittency exponent. This value turns out to be the same as the one observed by Gotoh et al. in their DNS. Since Bodenschatz assigned $Re = 31\,400$ with the formula (4), $\eta = 30.3\ \mu\text{m}$ gives $\ell_{\text{in}} = 0.071\ \text{m}$, as it should be. Therefore, in this case, we see that the energy-input scale is equal to the integral length scale, i.e., $\ell_{\text{in}} = \ell_0$, and that $\bar{n} = n = 17.1$.

7 Discussions

A comparison of the PDF's of accelerations are put in Fig. 5 on (a) log and (b) linear scale. The thin and the thick lines are those theoretical PDF's in Fig. 2 and in Fig. 3, respectively. The analysis of the data by Bodenschatz for the accelerations in terms of the log-normal model was performed just the same way as the multifractal analysis to get $\mu = 0.260$ and $n = 15.5$. The resulting PDF is given by dashed line which deviates slightly upward for larger values of ω_n compared with the thin line. This deviation can be understood from the scaling exponents ζ_m of the velocity structure function within the log-normal model. It becomes negative for larger values of m . The dotted line is the empirical PDF given by Bodenschatz et al. [25] which deviate downward for larger values of ω_n . The dotted-dashed line is the PDF given by Beck [35] for the studies both of the PDF's by Bodenschatz et al. and of Gotoh et al.. The lines other than the theoretical PDF's in Fig. 5 give rather poor explanations at the center part.

From the above analyses of two experiments, we reveal that there are two mechanisms contributing to the PDF of the accelerations, i.e, one is for the tail part, and the other for the center part. The structure of the PDF $\hat{\Lambda}^{(n)}(\omega_n)$ for the tail part, $\omega_n^\dagger \leq |\omega_n|$, is given by (40) that represents the intermittent large deviations which is a manifestation of the multifractal distribution of singularities in physical space due to the scale invariance of the Navier-Stokes equation for large Reynolds number. The experiment conducted by Bodenschatz et al. [23,24] visualized the singularities in physical space by tracing the "fluid particle" in turbulence. The specific form (40) comes from the distribution function for the singularity exponent α that is represented by the Tsallis-type distribution function (13) with the parameter q which is determined by the observed value of the intermittency exponent. The flatness of the PDF mainly provides us with the information of this tail part. The structure of

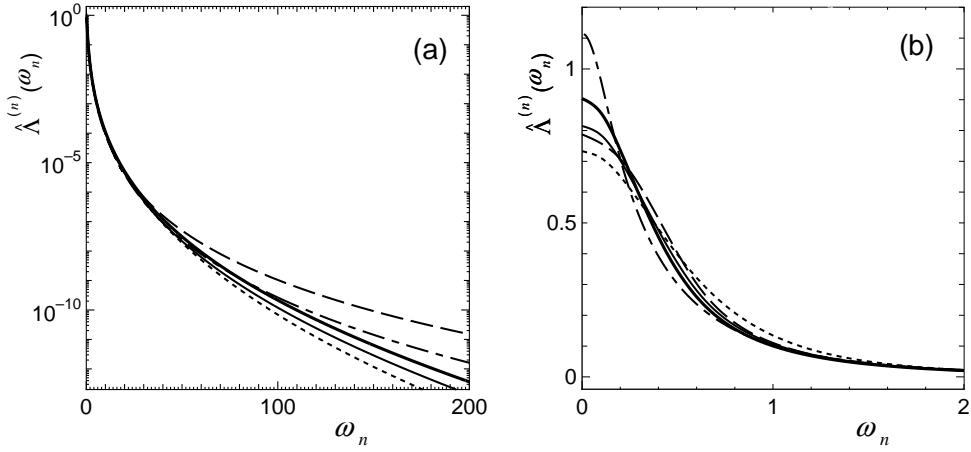


Fig. 5. Comparison of PDF's of accelerations on (a) log and (b) linear scale. The thin and thick lines are, respectively, the theoretical PDF's in Fig. 2 and Fig. 3. The dashed line represents the PDF within the log-normal model, and the dotted line does the empirical PDF given by Bodenschatz et al.. The dotted-dashed line is the PDF given by Beck [35].

the PDF for the center part, $|\omega_n| \leq \omega_n^\dagger$, is given by (43) that represents small deviations violating the scale invariance due to thermal fluctuations and/or observation error. The PDF for this part is assumed to be given by the Tsallis-type distribution function for acceleration itself with the parameter q' . In this paper, the value of q' are determined with the help of the experimentally observed PDF at the center part, giving $q' = 1.45$ and $q' = 1.7$ which is close to 1.5 proposed by Beck [31,32]. The value of q' should be determined by investigating the dynamics of thermal fluctuations and/or observation error on the multifractal support, which may have non-additive character. This is one of the attractive future problems. Note that we already saw that $1/(q' - 1)$ depends on r/η , linearly, through the study of the PDF's of velocity fluctuations, a detailed of which will be reported elsewhere. The tail part and the center part are separated at $\omega_n^\dagger \approx 0.6$. This gives $\alpha^\dagger \approx 1$ that satisfies the condition $\alpha < 1.5$ in which the singularity appears in fluid particle accelerations.

We saw that the PDF's derived within the multifractal analysis seem to be sensitive to the characteristic lengths such as the distance of two measuring points, the space resolution in measurement and the mesh size of DNS. We also knew that the multifractal distribution of singularities in physical space, on which the present analysis rests, is robust enough to allow us to apply the multifractal analysis to the ranges outside of the inertial range. How to put the information of energy-input scale into the multifractal analysis is one of the important future problems. It may be resolved when one succeeds to reveal the dynamical foundation underlying the basis of the multifractal analysis, starting an investigation by the stochastic Navier-Stokes equation with the energy input term. If one could put the stochastic Navier-Stokes equation

under the influence of white Gaussian noise, describing thermal fluctuation related to kinematic viscosity, into a linealized stochastic equation with a renormalized turbulent viscosity [36], the relevant stochastic process should be the one related to the PDF of accelerations derived in this paper, which may be named *Rényi* or *Tsallis process*. The success of the multifractal analysis in the studies of experimental PDF's may indicate that the multifractal distribution of singularities in physical space are robust against the addition of the energy-input term.

The present multifractal analysis may open new aspect for the systems with large deviation found in a large variety of areas (see, for example, the web site in [12]). Among them, an application of the multifractal analysis to vortex tangle [37] in ^4He and ^3He is one of the exciting future problems. In low temperature, the tail part of PDF comes from the singularity in the superfluid component within the two fluid model. Whereas, the value of q' for the center part of PDF may be determined by the dynamical structure of quantized vortices.

Acknowledgements

The authors would like to thank Prof. R.H. Kraichnan for his critical and enlightening comments, and Prof. C. Tsallis for his fruitful comments with encouragement. The authors are grateful to Prof. E. Bodenschatz and Prof. T. Gotoh for the kindness to show their data prior to publication.

References

- [1] T. Arimitsu and N. Arimitsu, Phys. Rev. E **61** (2000) 3237.
- [2] T. Arimitsu and N. Arimitsu, J. Phys. A: Math. Gen. **33** (2000) L235 [CORRIGENDUM: **34** (2001) 673].
- [3] T. Arimitsu and N. Arimitsu, Chaos, Solitons and Fractals **13** (2002) 479.
- [4] T. Arimitsu and N. Arimitsu, Prog. Theor. Phys. **105** (2001) 355.
- [5] T. Arimitsu and N. Arimitsu, Physica A **295** (2001) 177.
- [6] N. Arimitsu and T. Arimitsu, J. Korean Phys. Soc. **40** (2001) 1032.
- [7] T. Arimitsu and N. Arimitsu, Physica A **305** (2002) 218.
- [8] T. Arimitsu and N. Arimitsu, J. Phys.: Condens. Matter **14** (2002) 2237.
- [9] N. Arimitsu and T. Arimitsu, Europhys. Lett. **60** (2002) 60.

- [10] T. Arimitsu and N. Arimitsu, (2003) [cond-mat/0301516].
- [11] C. Tsallis, *J. Stat. Phys.* **52** (1988) 479.
- [12] C. Tsallis, *Braz. J. Phys.* **29** (1999) 1; On the related recent progresses see at <http://tsallis.cat.cbpf.br/biblio.htm>.
- [13] A. Rényi, *Proc. 4th Berkeley Symp. Maths. Stat. Prob.* **1** (1961) 547.
- [14] J.H. Havrda and F. Charvat, *Kybernetika* **3** (1967) 30.
- [15] A.N. Kolmogorov, *C.R. Acad. Sci. USSR* **30** (1941) 301; 538.
- [16] A.M. Oboukhov, *J. Fluid Mech.* **13** (1962) 77.
- [17] A.N. Kolmogorov, *J. Fluid Mech.* **13** (1962) 82.
- [18] A.M. Yaglom, *Sov. Phys. Dokl.* **11** (1966) 26.
- [19] U. Frisch, P-L. Sulem and M. Nelkin, *J. Fluid Mech.* **87** (1978) 719.
- [20] C. Meneveau and K. R. Sreenivasan, *Phys. Rev. Lett.* **59** (1987) 1424.
- [21] C. Meneveau and K. R. Sreenivasan, *Nucl. Phys. (Proc. Suppl.) B* **2** (1987) 49.
- [22] I. Hosokawa, *Phys. Rev. Lett.* **66** (1991) 1054.
- [23] A. La Porta, G. A. Voth, A. M. Crawford, J. Alexander and E. Bodenschatz, *Nature* **409** (2001) 1017.
- [24] G. A. Voth, A. La Porta, A. M. Crawford, J. Alexander and E. Bodenschatz, *Nature* **469** (2001) 121.
- [25] A. M. Crawford, N. Mordant and E. Bodenschatz, (2002) physics/0212080.
- [26] T. Gotoh, private communication
- [27] T. Gotoh, D. Fukayama and T. Nakano, *Phys. Fluids* **14** (2002) 1065.
- [28] U. Frisch and G. Parisi, in *Turbulence and Predictability in Geophysical Fluid Dynamics and Climate Dynamics*, ed. by M. Ghil, R. Benzi and G. Parisi (North-Holland, New York, 1985) 84.
- [29] U.M.S. Costa, M.L. Lyra, A.R. Plastino and C. Tsallis, *Phys. Rev. E* **56** (1997) 245.
- [30] M.L. Lyra and C. Tsallis, *Phys. Rev. Lett.* **80** (1998) 53.
- [31] C. Beck, *Phys. Lett.* **287** (2001) 240.
- [32] C. Beck, *Physica A* **306** (2002) 189.
- [33] G.S. Lewis and H.L. Swinney, *Phys. Rev. E* **59** (1999) 5457.
- [34] Communications with Prof. R.H. Kraichnan and Prof. T. Gotoh.
- [35] C. Beck, (2002) cond-mat/0212566.

- [36] W. Heisenberg, Z. Phys. **124** (1948) 628.
- [37] R. P. Feynman, *Progress in Low Temperature Physics* ed. by C. J. Gorter (Amsterdam: North Holland, 1955) 17.